JACS
JOURNAL OF THE AMERICAN CHEMICAL SOCIETY

Article

pubs.acs.org/JACS

Structural Insights into the Post-Chemistry Steps of Nucleotide Incorporation Catalyzed by a DNA Polymerase

Andrew J. Reed,[†,‡,§] Rajan Vyas,[†,§] Austin T. Raper,[†,‡] and Zucai Suo*[,†,‡]

[†]Department of Chemistry and Biochemistry and [‡]The Ohio State Biochemistry Program, The Ohio State University, Columbus, Ohio 43210, United States

Supporting Information

ABSTRACT: DNA polymerases are essential enzymes that faithfully and efficiently replicate genomic information.[1−3] The mechanism of nucleotide incorporation by DNA polymerases has been extensively studied structurally and kinetically, but several key steps following phosphodiester bond formation remain structurally uncharacterized due to utilization of natural nucleotides. It is thought that the release of pyrophosphate (PP_i) triggers reverse conformational changes in a polymerase in order to complete a full catalytic cycle as well as prepare for DNA translocation and subsequent incorporation events. Here, by using the triphosphates of chain-terminating antiviral drugs lamivudine ((-)3TC-TP) and emtricitabine ((-)FTC-TP), we structurally reveal the correct sequence of post-chemistry steps during nucleotide incorporation by human DNA polymerase β (hPolβ) and provide a structural basis for PP_i release. These post-catalytic structures reveal hPolβ in an open conformation with PP_i bound in the active site, thereby strongly suggesting that the reverse conformational changes occur prior to PP_i release. The results also help to refine the role of the newly discovered third divalent metal ion for DNA polymerase-catalyzed nucleotide incorporation. Furthermore, a post-chemistry structure of hPolβ in the open conformation, following incorporation of (-)3TC-MP, with a second (-)3TC-TP molecule bound to the active site in the absence of PP_i, suggests that nucleotide binding stimulates PP_i dissociation and occurs before polymerase translocation. Our structural characterization defines the order of the elusive post-chemistry steps in the canonical mechanism of a DNA polymerase.

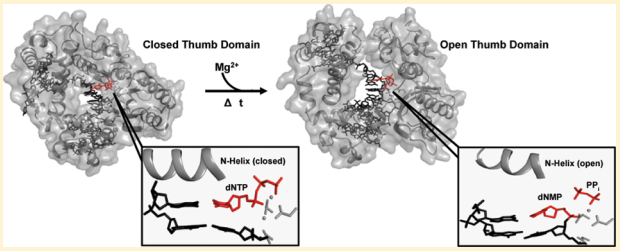

INTRODUCTION

DNA polymerases (Pols) are intricate cellular machines capable of synthesizing genomic DNA in an efficient and faithful manner. In general, Pols from all six families contain three canonical polymerase domains, the fingers, thumb, and palm, arranged in a right-hand configuration.[2,4] In addition to structural similarities, Pols catalyze DNA synthesis through a largely conserved mechanism of nucleotide incorporation following DNA binding, wherein a nucleotide is selected, bound, and subsequently incorporated into DNA (Scheme 1).[1−3] Accordingly, the products of nucleotide incorporation by Pols include an extended DNA primer and pyrophosphate (PP_i). Global conformational changes upon nucleotide binding, such as an open → closed transition of the fingers domain for most Pols, or the thumb domain for human DNA polymerase beta (hPolβ), and a closed → open transition following nucleotide incorporation have been shown to act as fidelity checkpoints for Pols, influencing both nucleotide selectivity and catalytic efficiency.[5,6] Beyond these large conformational changes, more subtle motions that take place within individual Pol domains are suggested to be important for DNA and nucleotide binding, as well as nucleotide incorporation.[6]

While a great deal of biochemical, biophysical, and structural work has focused on characterizing the steps up to and including phosphodiester bond formation,[1,2] little structural work has investigated the steps occurring after catalysis, such as PP_i release, reverse conformational changes, and either DNA translocation or dissociation (Scheme 1). Although these steps are key determinants in Pol processivity and likely control the balance between the competing polymerization and editing (i.e., exonuclease) activities of Pols,[1,5,7] characterization of these events is problematic, as these steps are rapid during natural nucleotide incorporation.[8] Accordingly, it remains unclear if PP_i release occurs first, to effectively trigger the reverse conformational changes of the Pol, or the reverse conformational changes occur first, allowing PP_i to simply diffuse out of the active site. Furthermore, it is unclear what roles various active site residues, metal ions, and an incoming nucleotide serve in these post-chemistry steps. Here, we utilized the triphosphate derivatives of lamivudine ((-)3TC-TP) and emtricitabine ((-)FTC-TP) to structurally characterize the elusive post-chemistry steps of DNA polymerase-catalyzed nucleotide incorporation. Despite their L-stereochemistry, sulfur-substituted ribose, and lack of a 3′-OH (Figure S1), these unnatural nucleotides form natural Watson−Crick base pairs with the templating base, adopt productive triphosphate conformations, and can be utilized by hPolβ, albeit with altered incorporation

Received: October 28, 2016
Published: December 13, 2016

DOI: 10.1021/jacs.6b11258
J. Am. Chem. Soc. 2017, 139, 465−471

Scheme 1. Canonical Mechanism of Nucleotide Incorporation for DNA Polymerases[a]

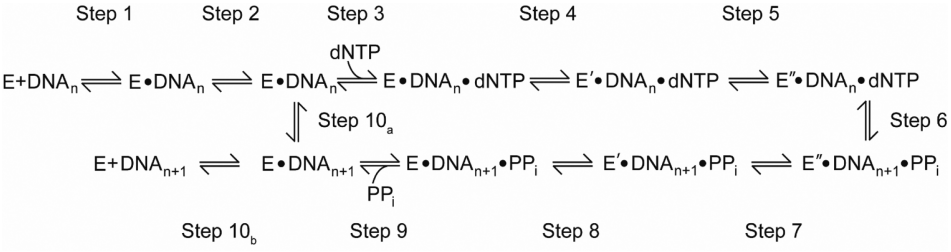

[a]E, E′, and E″ represent three different conformations of a polymerase sampled during correct nucleotide incorporation.

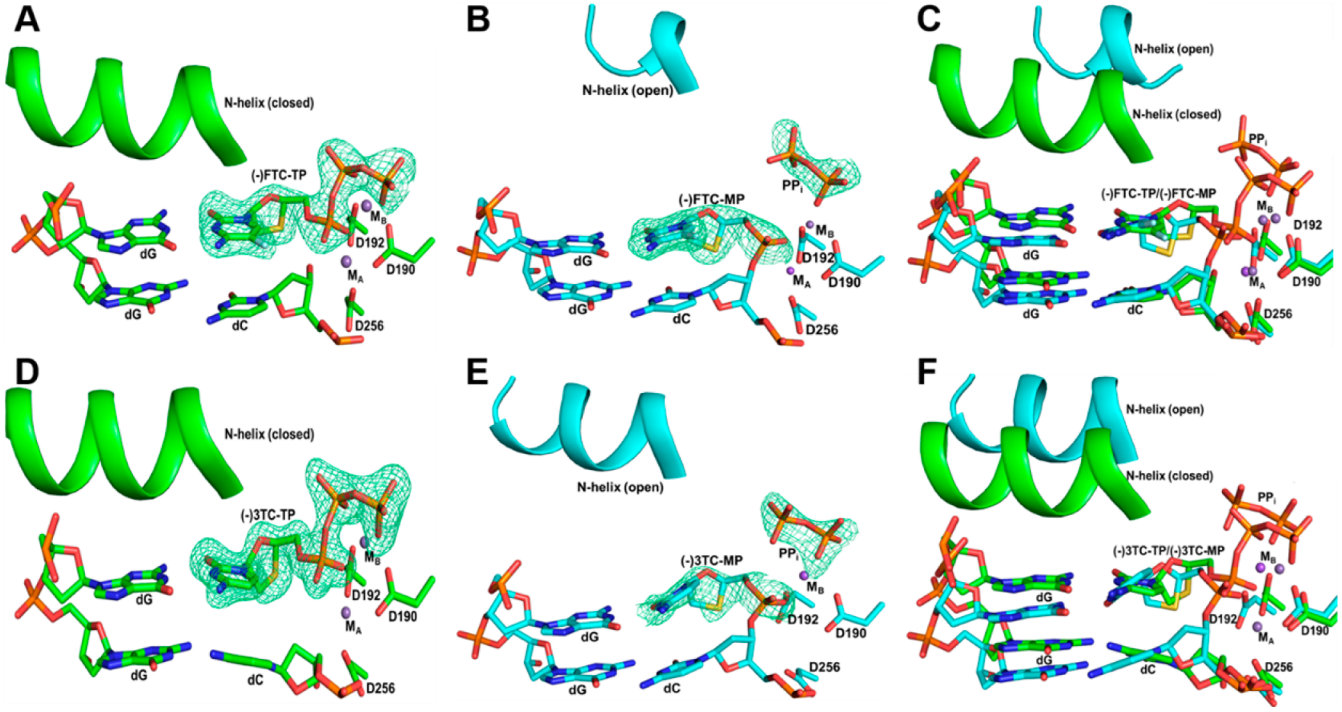

Figure 1. Active site views of bound and incorporated L-nucleotides. (A) Closed pre-catalytic ternary complex of hPolβ•DNA•(-)FTC-TP. (B) Open post-catalytic ternary complex of hPolβ•DNA−(-)FTC-MP•PP$_i$. (C) Superposition of structures presented in parts A and B. (D) Closed pre-catalytic ternary complex of hPolβ•DNA•(-)3TC-TP. (E) Open post-catalytic ternary complex of hPolβ•DNA−(-)3TC-MP•PP$_i$. (F) Superposition of structures presented in parts D and E. The N-helix is shown as a cartoon model. The metal ions, represented as spheres, are modeled as Mn^{2+} (M_A) and Mn^{2+} (M_B) in parts A and D, Na^+ (M_A) and Mn^{2+} (M_B) in part B, and Na^+ (M_B) in part E. The side chains of D190, D192, and D256 are shown as sticks. The F_o-F_c omit map (3σ) is displayed as green mesh.

kinetics.[9] Collectively, the unique properties offered by these nucleotide analogues, including their near natural configurations and interactions within the hPolβ active site, as well as their ability to prevent subsequent primer extension following slow incorporation, permitted us to capture the first glimpse of mechanistic steps following phosphodiester bond formation.

RESULTS AND DISCUSSION

Previous structural studies have been unable to characterize the post-chemistry steps with natural nucleotides due to rapid reverse protein conformational changes and PP$_i$ release.[1,2,10−14] To gain insight into the post-chemistry processes, we crystallized ternary complexes of hPolβ, DNA, and (-)3TC-TP (hPolβ•DNA•(-)3TC-TP) or (-)FTC-TP (hPolβ•DNA•(-)FTC-TP), the triphosphates of two highly successful antivrial drugs, lamivudine and emtricitabine, respectively, in the presence of Ca^{2+} followed by *in crystallo* Mn^{2+} exchange for 5 h. Unexpectedly, there was no observed nucleotide incorporation even after complete Ca^{2+} to Mn^{2+} exchange, likely due to slow L-nucleotide incorporation catalyzed by hPolβ.[9] These pre-catalytic ternary crystals yielded structures at resolutions of 2.49 and 2.00 Å (Table S1) for hPolβ•DNA•(-)FTC-TP (Figure 1A) and hPolβ•DNA•(-)3TC-TP (Figure 1D), respectively, with similar overall tertiary structures (rmsd of 0.78 and 0.72 Å, respectively) compared to the ternary structure of hPolβ, DNA, and natural dCTP (PDB code 4KLD)[10] (Figure S2), including a fully closed thumb domain. In addition, the pre-catalytic ternary structures have well-defined electron density for the incoming nucleotide and exhibit similar active site architecture compared to hPolβ•DNA•dCTP, except for a slight repositioning of A-site (M_A) and B-site (M_B) metal ions (Figure S2A). The hPolβ•DNA•(-)3TC-TP and hPolβ•DNA•(-)FTC-TP structures with Mn^{2+} likely represent E″•DNA$_n$•dNTP in Scheme 1.

Crystals of the pre-catalytic ternary complexes were then soaked in a Mn^{2+} or Mg^{2+} solution overnight to obtain post-catalytic structures. The crystals of hPolβ•DNA−(-)FTC-MP•PP$_i$ in the presence of Mg^{2+} (Figure 1B) and

DOI: 10.1021/jacs.6b11258
J. Am. Chem. Soc. 2017, 139, 465−471

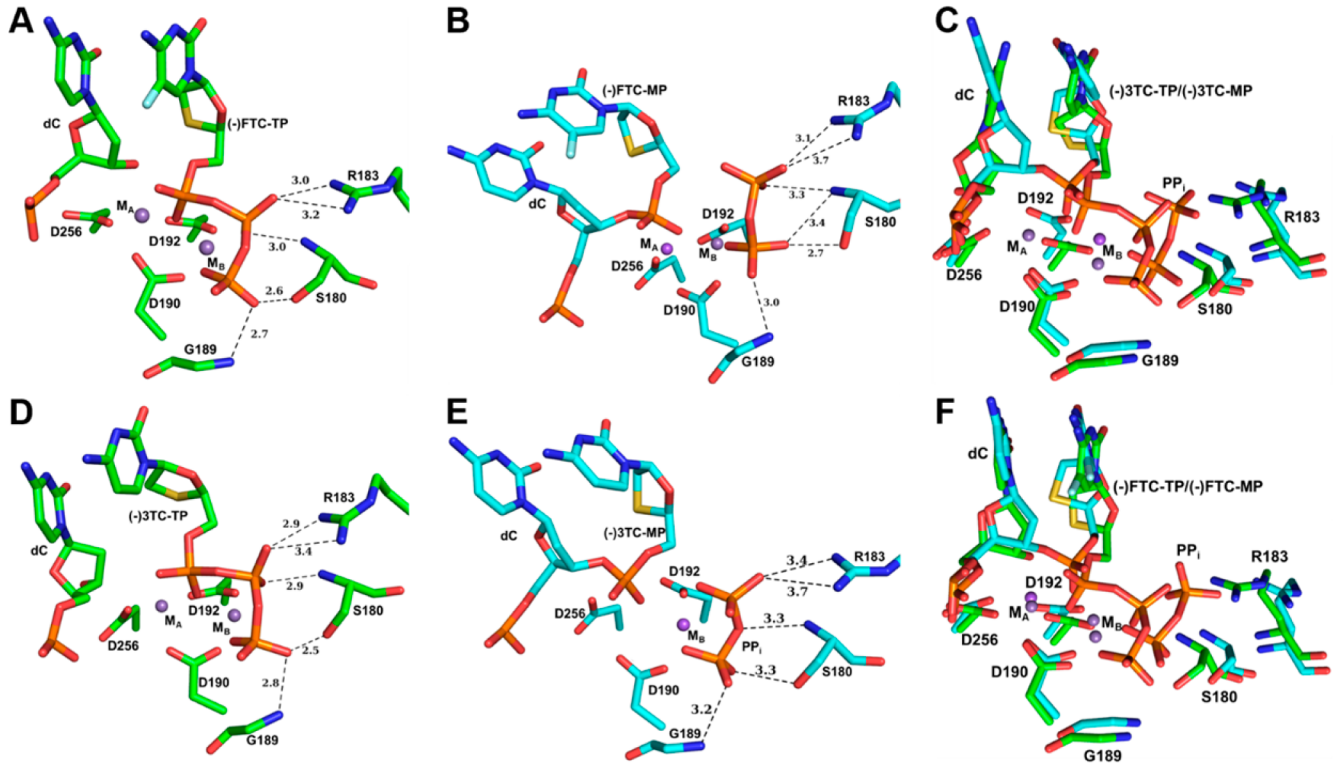

Figure 2. Zoomed interactions of the triphosphate of a nucleotide or the product pyrophosphate with palm domain residues. (A) Closed pre-catalytic ternary complex of hPolβ•DNA•(-)FTC-TP. (B) Open post-catalytic ternary complex of hPolβ•DNA−(-)FTC-MP•PP_i. (C) Superposition of structures presented in parts A and B. (D) Closed pre-catalytic ternary complex of hPolβ•DNA•(-)3TC-TP. (E) Open post-catalytic ternary complex of hPolβ•DNA−(-)3TC-MP•PP_i. (F) Superposition of structures presented in parts D and E. In all panels, the triphosphate or pyrophosphate forms hydrogen bonds (dashes) with the backbone nitrogen atoms of G189 and S180 and the side chains of R183 and S180. Distances are given in Å. The metal ions, represented as spheres, are modeled as Mn^{2+} (M_A) and Mn^{2+} (M_B) in parts A and D, Na^+ (M_A) and Mn^{2+} (M_B) in part B, and Na^+ (M_B) in part E. The active site residues are shown as sticks.

hPolβ•DNA−(-)3TC-MP•PP_i in the presence of Mn^{2+} (Figure 1E) diffracted to a resolution of 2.39 and 2.49 Å, respectively (Table S1). The active sites of both structures clearly indicate the formation of a covalent linkage between the terminal primer nucleotide, dC, and the monophosphates of lamivudine and emtricitabine, (-)FTC-MP or (-)3TC-MP (Figure 1B and E). Notably, in the hPolβ•DNA−(-)3TC-MP•PP_i structure (Figure 1E), the catalytic A-site metal ion is absent and the nucleotide binding B-site metal ion is modeled as Na^+, while they are modeled as Na^+ and Mn^{2+}, respectively, in the hPolβ•DNA−(-)FTC-MP•PP_i (Figure 1B). Further comparison between the active sites of hPolβ•DNA−(-)3TC-MP•PP_i and hPolβ•DNA−(-)FTC-MP•PP_i reveals that the B-site metal ions are in nearly identical positions and are associated with the newly generated PP_i (Figure 1B,E and Figure S3).

The overall tertiary structures of these post-catalytic ternary complexes are similar, with the N-helix adopting an open protein conformation, and overlay well with the binary structures, hPolβ•DNA and hPolβ•DNA_{nicked} (PDB codes 1BPX and 1BPZ, respectively),[15] except for the base portion of (-)3TC-TP, which forms a nonplanar Watson−Crick base pair with the templating nucleotide (Figure S3). Surprisingly, the product PP_i is also bound in the active site (Figures 1B and E and 2B and E) unlike previous post-catalytic structures wherein PP_i had been released.[10,11,14] Moreover, PP_i forms hydrogen bonds with several palm domain residues that are consistent with those seen in the closed, pre-catalytic ternary complexes (Figure 2). Previously, we have shown that, following nucleotide incorporation opposite 8-oxoguanine (8-oxoG), hPolβ is in the closed conformation with PP_i bound, but following extended incubation periods, hPolβ is observed in the open conformation with PP_i released.[14] Interestingly, a similar time-dependent structural study observing dCTP incorporation by hPolβ on undamaged DNA could not capture PP_i release or the reverse conformational change even 11 h after reaction initiation.[10] Furthermore, post-catalytic structures with T7 RNA polymerase[16] were unable to define the sequence of PP_i release and the closed → open conformational change. Clearly, the timing and the rapid kinetics of these post-chemistry processes are ambiguous and have likely contributed to poor structural characterization to date.

Here, the hPolβ•DNA−(-)3TC-MP•PP_i and hPolβ•DNA−(-)FTC-MP•PP_i structures are observed in an open conformation with PP_i bound (Figures 1B and E and 2B and E), which is surprising given that computational analyses of DNA polymerase I from *Bacillus stearothermophilus* (BF) have shown that PP_i release triggers post-catalytic conformational changes.[17] These open post-catalytic structures suggest a mechanism where PP_i can stay tightly associated with the polymerase active site following the reverse conformational change of the N-helix in the absence of the next nucleotide. Furthermore, this mechanism of PP_i release following a closed → open conformational change is supported by the persistent hydrogen bonding network between the β- and γ-phosphates of the nucleotides or the product PP_i and residues in the palm domain (Figure 2), which may also impede binding of the next nucleotide.

DOI: 10.1021/jacs.6b11258
J. Am. Chem. Soc. 2017, 139, 465−471

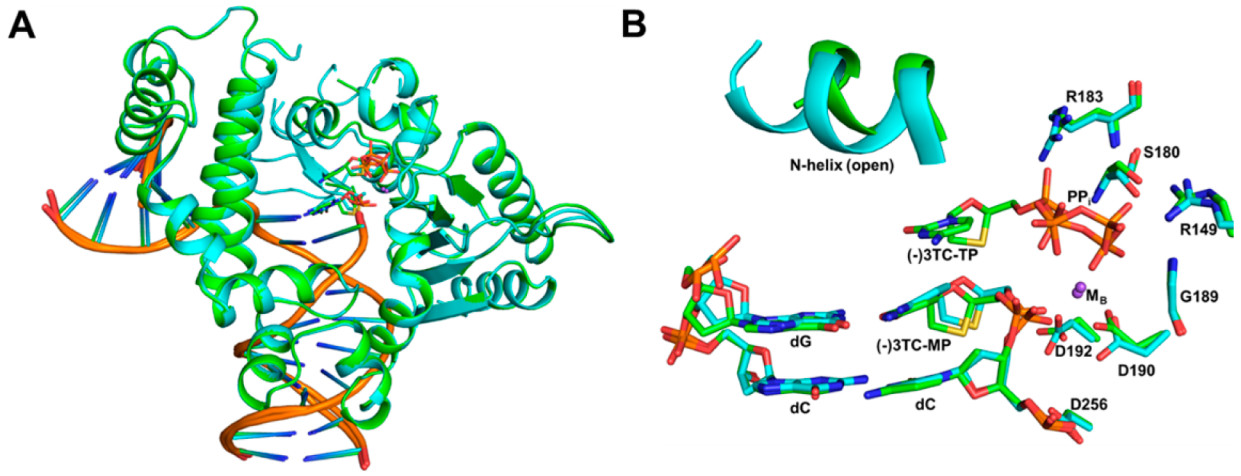

Figure 3. Superposition of post-catalytic structures of hPolβ with the phosphate forms of (-)3TC. Overall superposition of the hPolβ•DNA−(-)3TC-MP•PP_i (cyan) and hPolβ•DNA−(-)3TC-MP•(-)3TC-TP (green) structures. Between the two structures, the DNA substrate and protein backbone overlay well, respectively, with only a slight difference in the position of the N-heilx. (B) Active site superposition of the hPolβ•DNA−(-)3TC-MP•PP_i (cyan) and hPolβ•DNA−(-)3TC-MP•(-)3TC-TP (green) structures. The side chains (R183 and S180) and backbone atoms (G189 and S180) have similar interactions with PP_i and the triphosphate of (-)3TC-TP. The incoming (-)3TC-TP also has an additional interaction with R149 due to a slight repositioning of the γ-phosphate of (-)3TC-TP compared to PP_i.

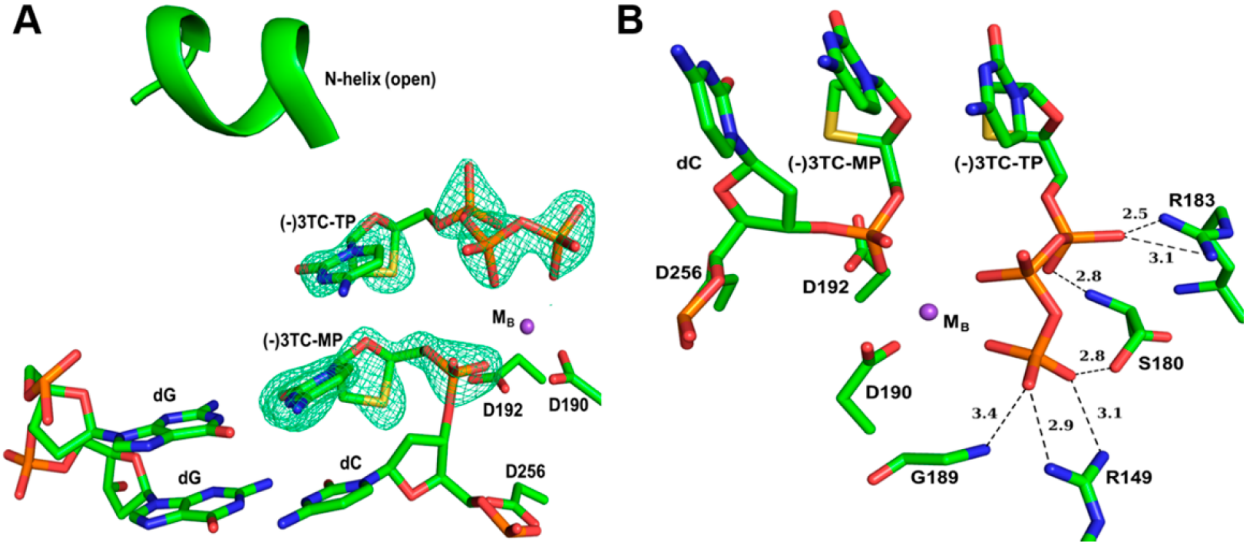

Figure 4. Zoomed active site views of the post-catalytic hPolβ•DNA−(-)3TC-MP•(-)3TC-TP structure. (A) (-)3TC-TP bound in the open conformation following (-)3TC-MP incorporation. The N-helix is shown as a cartoon model. The F_o−F_c map (3σ) is shown as green mesh. (B) Interactions of the bound (-)3TC-TP with palm domain residues. Hydrogen bonds (dashes with distances given in Å) are formed with the backbone nitrogen atoms of G189 and S180 and the side chains of R183 and S180. Two unique hydrogen bonds are formed between the triphosphate of (-)3TC-TP and the side chain of R149. In both panels, the B-site (M_B) metal ion, shown as a sphere, is modeled as Mn^{2+}. The active site residues are represented as sticks.

While examination of the DNA polymerase mechanism with natural substrates is preferred, the rapid kinetics associated with certain steps render structural characterization difficult or impossible. Fortuitously, our use of the chain-terminating nucleotide analogues has permitted the capture of the elusive post-chemistry events to further clarify the catalytic mechanism of hPolβ (Figures 1−3 and Scheme 1). Consistently, a kinetic study of human DNA polymerase γ (hPolγ) incorporating the triphosphate of another chain-terminating nucleotide analogue, 3′-azido-2′,3′-dideoxythymidine (AZT-TP), demonstrated that PP_i release following AZT-TP incorporation is slow,[18] suggesting the existence of a stable hPolγ•DNA−AZT-MP•PP_i complex.

In terms of the overall kinetic mechanism (Scheme 1), the above closed and open post-catalytic structures help to define steps 8 and 9, respectively. The pre-catalytic and chemistry steps (Scheme 1, steps 1−6) of nucleotide incorporation by hPolβ have been previously investigated structurally and kinetically, and we will not discuss them here.[19−21] However, we point out that step 4 in Scheme 1 represents the forward open → closed conformational transition of the thumb domain for hPolβ, which already happened in the crystals prior to the metal ion exchange experiments described in this study. Steps 5−7 of Scheme 1 occurred following metal ion exchange but were not observed *in crystallo*. Notably, step 7 of Scheme 1 represents the reverse of the conformational changes (i.e., E″ → E′) in the active site of hPolβ that occurred during step

DOI: 10.1021/jacs.6b11258
J. Am. Chem. Soc. 2017, 139, 465−471

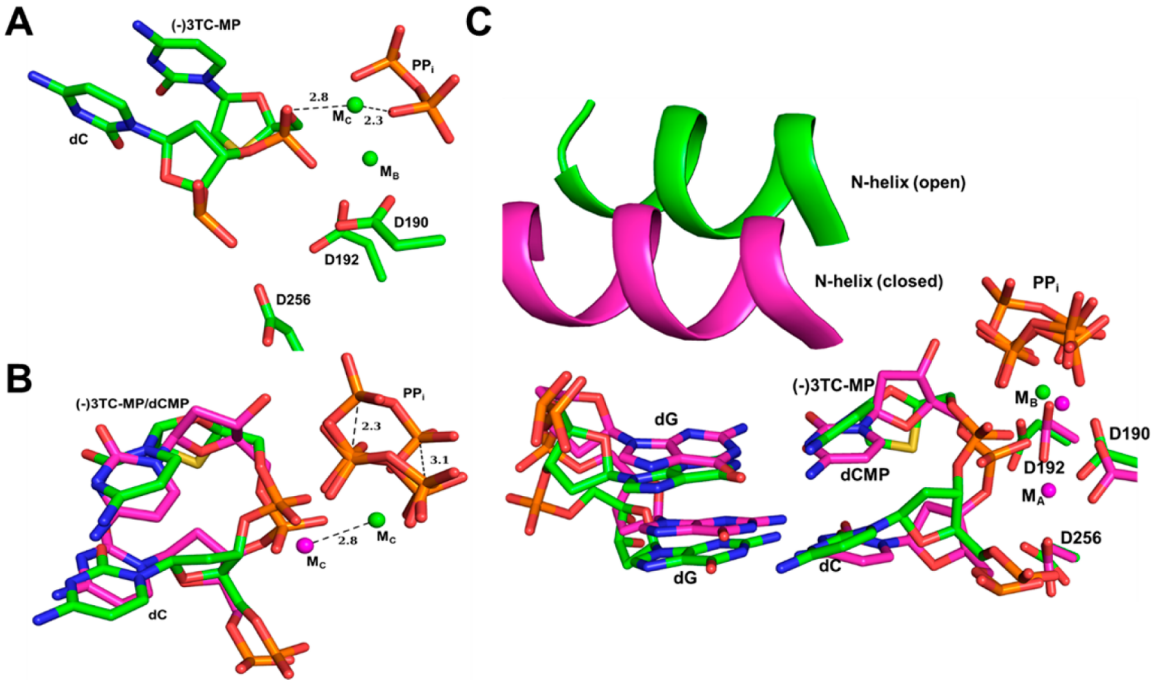

Figure 5. Evidence for a third metal ion following (-)3TC-TP incorporation. (A) Stick model of the zoomed hPolβ•DNA−(-)3TC-MP•PP_i structure with both the B-site (M_B) and C-site (M_C) metal ions shown as spheres and modeled as Na^+ ions. Ligands for the C-site metal ion are shown as dashes with distances in Å. (B and C) Superposition of the hPolβ•DNA−(-)3TC-MP•PP_i structure and the structure of hPolβ following normal dCTP incorporation (hPolβ•DNA−dCMP•PP_i, PDB code 4KLG). Metal ions for the hPolβ•DNA−dCMP•PP_i structure are modeled as Mg^{2+} ions. (B) Movement of the C-site metal ion (M_C) and PP_i following domain reopening is shown as dashes with distances in Å. The M_C ion for the hPolβ•DNA−(-)3TC-MP•PP_i structure is modeled as Na^+ based on the ligand distances and the concerted movement of M_C and PP_i. (C) Overall active site superposition demonstrating the change in the N-helix and similar positions of catalytic aspartate residues and the DNA template strand.

5,[21,22] but our structures here do not inform on these events. Following nucleotide binding and incorporation, our post-catalytic ternary structures of hPolβ (Figures 1B and E and 2B and E) strongly suggest that the thumb domain must first complete the reverse, closed → open transition (Scheme 1, step 8) before PP_i can be released (Scheme 1, step 9). However, the sequence of the post-chemistry steps following a misincorporation event may be different than described here. For example, PP_i release following a misincorporation is purported to be fast, as shown in a time-resolved crystallographic study of hPolβ wherein only open-product complexes without PP_i, rather than closed-product complexes with bound PP_i, could be isolated following a misincorporation event.[10] This is consistent with kinetic studies of T7 DNA polymerase[8] and φ29 DNA polymerase,[23] wherein a mismatched primer terminus could not be removed via pyrophosphorolysis due to fast PP_i dissociation. In addition, the sequence of post-chemistry steps for natural nucleotide incorporation may or may not follow the sequence described here. However, structural characterization of such events may be unattainable due to the fast kinetics of correct, natural nucleotide incorporation. For example, our previous time-dependent studies viewing dCTP incorporation opposite 8-oxoG during hPolβ catalyzed translesion synthesis were unable to elucidate the order of events following chemistry.[14] To evaluate whether or not incorporation of a natural nucleotide or misincorporation follows the sequence of post-chemistry steps in Scheme 1, similar structural studies as presented here are required.

Clearly, the molecular determinants for the reverse conformational changes and pyrophosphate release have not been well understood structurally, but our results illuminate key details of these events for correct nucleotide incorporation. As proposed previously, it is possible that, rather than passive PP_i release and DNA translocation (Scheme 1, steps 9 and 10_a, respectively), the presence of the next correct nucleotide may actively displace PP_i during processive DNA synthesis. Therefore, during a subsequent nucleotide incorporation, PP_i dissociation may occur as late as step 3 in Scheme 1.[17,24,25] To investigate the role of nucleotide binding in PP_i release, crystals of hPolβ•DNA−(-)3TC-TP with Ca^{2+} were soaked in a cryosolution containing Mg^{2+} and (-)3TC-TP. Crystals of hPolβ•DNA−(-)3TC-MP•(-)3TC-TP diffracted to 1.85 Å resolution and showed the binding of the second (-)3TC-TP following the incorporation of the first (-)3TC-TP but the notable absence of PP_i generated during nucleotide incorporation (Figure 4). Surprisingly, (-)3TC-TP in the hPolβ•DNA−(-)3TC-MP•(-)3TC-TP structure forms a similar hydrogen bonding network with several residues (S180, R183, and G189) compared to PP_i in the hPolβ•DNA−(-)3TC-MP•PP_i structure (Figures 3B and 4B). In addition, (-)3TC-TP forms two hydrogen bonds with the side chain of R149 that further facilitate nucleotide binding and may aid in PP_i displacement (Figures 3B and 4B). This is consistent with several stopped-flow studies which demonstrated that in the presence of the next correct nucleotide PP_i release is fast, while in the absence of additional nucleotide the release is slow.[17,24,25] Furthermore, the hPolβ•DNA−(-)3TC-MP•(-)3TC-TP structure may suggest that the binding of the next nucleotide occurs before and provides energy for hPolβ translocation. This is contrary to the sequence of steps 10_a and 3 in the canonical mechanism (Scheme 1). We were able to capture such a metastable complex because the nicked DNA−(-)3TC-MP substrate

DOI: 10.1021/jacs.6b11258
J. Am. Chem. Soc. 2017, 139, 465−471

prevents hPolβ translocation, and the incoming (-)3TC-TP mismatch with the next nucleotide (dC) of the template would disfavor the strand-displacement activity of hPolβ.[26]

Alternatively, in the absence of the next correct nucleotide, PP_i release could be triggered or aided by protein side chain movements or water solvation that disrupts interactions between PP_i and protein side chains. Conversely, additional metal ions, such as the third divalent metal ion observed in recent time-resolved X-ray crystallography studies with Pols,[10−14] are unlikely to aid PP_i release. In the structures following nucleotide incorporation and reopening of the thumb domain, a third metal ion is only observed for the hPolβ•DNA−(-)3TC-MP•PP_i structure (Figures 1D−F and 5) but not with the hPolβ•DNA−(-)FTC-MP•PP_i (Figure 1A−C). In addition, the third metal ion and PP_i remain associated following chemistry, and together move upon reopening of the thumb domain when compared with the positions of the third divalent metal ion and PP_i in the structures of correct nucleotide incorporation with hPolβ (Figure 5A and B). Accordingly, these data limit the role of the third metal ion to catalytic events occurring during the chemistry step (step 6, Scheme 1). Despite the third metal ion remaining associated with PP_i immediately following chemistry, it dissociates first. This is further supported by the product structures of hPolβ with the correct nucleotide, wherein the third divalent metal ion is released prior to domain reopening.[10] This is contrary to the initial hypothesis that the third divalent metal acts as an exit shuttle for PP_i release.[13,14] However, for hPolη, it cannot be ruled out that the third divalent metal ion aids PP_i release due to the lack of post-catalytic structures with the third divalent metal ion released and PP_i still bound. Regardless of the mode in which PP_i release is triggered, it is clear that the release of this small molecule occurs independent of the major, reverse conformational changes of hPolβ.

CONCLUSION

In summary, we report five post-catalytic structures of human DNA polymerase β (hPolβ) following incorporation of the L-nucleotide analogues, (-)3TC-TP and (-)FTC-TP. Contrary to common belief, we observe the first structural evidence, to our knowledge, that the inevitable closed → open thumb domain transition following nucleotide incorporation occurs before PP_i release. Furthermore, the ternary structure in which an additional nucleotide is bound with a previously incorporated nucleotide suggests that the nucleotide binding to the complex following the closed → open conformational change may trigger PP_i release and initiate the next catalytic cycle.

EXPERIMENTAL SECTION

Preparation of Protein and DNA. Full-length hPolβ was overexpressed and purified as described previously.[14] DNA oligomers were purchased from Integrated DNA Technologies and were purified by denaturing polyacrylamide gel electrophoresis. Crystallization oligomers consisted of a 16-mer template (5′-CCGACGGCGCAT-CAGC-3′), a 10-mer upstream primer (5′-GCTGATGCGC-3′), and a 5-mer downstream 5′-phosphorylated primer (5′-pGTCGG-3′) as described previously.[10] For crystallization, the template, upstream primer, and downstream primer were mixed in a 1:1:1 ratio and annealed by heating to 95 °C for 5 min followed by slowly cooling to 4 °C to form the single-nucleotide gapped DNA substrate (1 mM). The L-nucleotides, (-)FTC-TP and (-)3TC-TP, were obtained from Jena Bioscience. If not specifically mentioned, all DNA substrates are single-nucleotide gapped. DNA_{nicked}, DNA−(-)3TC-MP, and DNA−(-)FTC-MP are nicked DNA substrates.

hPolβ Crystallization and Structure Determination. Purified human hPolβ was dialyzed into a buffer containing 50 mM NaOAc (pH 5.5), 75 mM NaCl, 5% glycerol, and 0.1 mM DTT and concentrated to 20 mg/mL as described previously.[27] Binary complexes (hPolβ•DNA) were prepared by mixing purified hPolβ and the single-nucleotide gapped DNA substrate (1 mM) in a 1:1 ratio at 4 °C followed by heating to 35 °C and subsequent cooling to room temperature.[28] Binary crystals were obtained by hanging drop vapor diffusion against a reservoir solution containing 50 mM imidazole, pH 7.5, 16−18% PEG3350, and 350 mM sodium acetate.[28] Binary crystals were then seeded into a freshly prepared ternary complex solution (hPolβ•DNA, 10 mM $CaCl_2$ and 2 mM (-)3TC-TP or (-)FTC-TP) to obtain pre-catalytic ternary crystals (hPolβ•DNA•(-)3TC-TP or hPolβ•DNA•(-)FTC-TP) at room temperature, as described previously.[15] The resulting pre-catalytic ternary crystals were then soaked in a cryosolution (15% ethylene glycol, 50 mM imidazole (pH 7.5), 20% PEG3350, 90 mM NaOAc) containing either Mg^{2+} or Mn^{2+} ions (50 mM) for 5 h to achieve thumb domain closure or overnight to allow nucleotide incorporation. Crystals were flash frozen in liquid nitrogen, and X-ray diffraction data were collected using the LRL-CAT beamline facilities at Advance Photon Source (APS), Argonne National Laboratory. The X-ray diffraction data were processed using MOSFLM.[29] Structures were solved by molecular replacement using PHASER.[30] A previous structure (PDB code: 4KLD),[10] devoid of ligands and solvent molecules, was used as the initial model. Structural refinement was carried out using REFMAC5.[31] COOT was used for visualization and model building.[32] The quality of the models was assessed using PROCHECK.[33] Figures were created using PYMOL.[34]

ASSOCIATED CONTENT

Supporting Information

The Supporting Information is available free of charge on the ACS Publications website at DOI: 10.1021/jacs.6b11258.

Supporting figures and crystallographic tables (PDF)

AUTHOR INFORMATION

Corresponding Author

*suo.3@osu.edu

ORCID

Rajan Vyas: 0000-0003-0264-446X

Zucai Suo: 0000-0003-3871-3420

Author Contributions

§A.J.R., R.V.: These authors contributed equally.

Notes

The authors declare no competing financial interest.

ACKNOWLEDGMENTS

We would like to thank Dr. Joy Feng of Gilead Sciences, Inc., for supplying the L-nucleotides used for crystallization. The research was supported by National Institutes of Health Grants ES024585 and ES026821 to Z.S. A.T.R. was supported by National Institutes of Health Training Grant T32GM008512. This research used resources of the Advanced Photon Source, a U.S. Department of Energy (DOE) Office of Science User Facility operated for the DOE Office of Science by Argonne National Laboratory under Contract No. DE-AC02-06CH11357. Use of the Lilly Research Laboratories Collaborative Access Team (LRL-CAT) beamline at Sector 31 of the Advanced Photon Source was provided by Eli Lilly Company, which operates the facility. Atomic coordinates and structure factors for the reported crystal structures have been deposited

DOI: 10.1021/jacs.6b11258
J. Am. Chem. Soc. 2017, 139, 465−471

with the Protein Data Bank with accession codes 5TB8, 5TB9, 5TBA, 5TBB, and 5TBC.

REFERENCES

(1) Joyce, C. M.; Benkovic, S. J. *Biochemistry* **2004**, *43*, 14317.
(2) Rothwell, P. J.; Waksman, G. *Adv. Protein Chem.* **2005**, *71*, 401.
(3) Fiala, K. A.; Abdel-Gawad, W.; Suo, Z. *Biochemistry* **2004**, *43*, 6751.
(4) Fowler, J. D.; Suo, Z. *Chem. Rev.* **2006**, *106*, 2092.
(5) Johnson, K. A. *Annu. Rev. Biochem.* **1993**, *62*, 685.
(6) Raper, A. T.; Suo, Z. *Biochemistry* **2016**, *55*, 5832.
(7) Johnson, S. J.; Beese, L. S. *Cell* **2004**, *116*, 803.
(8) Patel, S. S.; Wong, I.; Johnson, K. A. *Biochemistry* **1991**, *30*, 511.
(9) Brown, J. A.; Pack, L. R.; Fowler, J. D.; Suo, Z. *Antimicrob. Agents Chemother.* **2011**, *55*, 276.
(10) Freudenthal, B. D.; Beard, W. A.; Shock, D. D.; Wilson, S. H. *Cell* **2013**, *154*, 157.
(11) Freudenthal, B. D.; Beard, W. A.; Perera, L.; Shock, D. D.; Kim, T.; Schlick, T.; Wilson, S. H. *Nature* **2015**, *517*, 635.
(12) Gao, Y.; Yang, W. *Science* **2016**, *352*, 1334.
(13) Nakamura, T.; Zhao, Y.; Yamagata, Y.; Hua, Y. J.; Yang, W. *Nature* **2012**, *487*, 196.
(14) Vyas, R.; Reed, A. J.; Tokarsky, E. J.; Suo, Z. *J. Am. Chem. Soc.* **2015**, *137*, 5225.
(15) Sawaya, M. R.; Prasad, R.; Wilson, S. H.; Kraut, J.; Pelletier, H. *Biochemistry* **1997**, *36*, 11205.
(16) Yin, Y. W.; Steitz, T. A. *Cell* **2004**, *116*, 393.
(17) Golosov, A. A.; Warren, J. J.; Beese, L. S.; Karplus, M. *Structure* **2010**, *18*, 83.
(18) Hanes, J. W.; Johnson, K. A. *Nucleic Acids Res.* **2007**, *35*, 6973.
(19) Beard, W. A.; Wilson, S. H. *Chem. Rev.* **2006**, *106*, 361.
(20) Balbo, P. B.; Wang, E. C.; Tsai, M. D. *Biochemistry* **2011**, *50*, 9865.
(21) Towle-Weicksel, J. B.; Dalal, S.; Sohl, C. D.; Doublie, S.; Anderson, K. S.; Sweasy, J. B. *J. Biol. Chem.* **2014**, *289*, 16541.
(22) Murphy, D. L.; Jaeger, J.; Sweasy, J. B. *J. Am. Chem. Soc.* **2011**, *133*, 6279.
(23) Blasco, M. A.; Bernad, A.; Blanco, L.; Salas, M. *J. Biol. Chem.* **1991**, *266*, 7904.
(24) Johnson, R. S.; Strausbauch, M.; Carraway, J. K. *J. Mol. Biol.* **2011**, *412*, 849.
(25) Zhao, L.; Pence, M. G.; Eoff, R. L.; Yuan, S.; Fercu, C. A.; Guengerich, F. P. *FEBS J.* **2014**, *281*, 4394.
(26) Prasad, R.; Lavrik, O. I.; Kim, S. J.; Kedar, P.; Yang, X. P.; Vande Berg, B. J.; Wilson, S. H. *J. Biol. Chem.* **2001**, *276*, 32411.
(27) Pelletier, H.; Sawaya, M. R.; Wolfle, W.; Wilson, S. H.; Kraut, J. *Biochemistry* **1996**, *35*, 12742.
(28) Batra, V. K.; Beard, W. A.; Shock, D. D.; Krahn, J. M.; Pedersen, L. C.; Wilson, S. H. *Structure* **2006**, *14*, 757.
(29) Battye, T. G.; Kontogiannis, L.; Johnson, O.; Powell, H. R.; Leslie, A. G. *Acta Crystallogr., Sect. D: Biol. Crystallogr.* **2011**, *67*, 271.
(30) McCoy, A. J.; Grosse-Kunstleve, R. W.; Adams, P. D.; Winn, M. D.; Storoni, L. C.; Read, R. J. *J. Appl. Crystallogr.* **2007**, *40*, 658.
(31) Murshudov, G. N.; Skubak, P.; Lebedev, A. A.; Pannu, N. S.; Steiner, R. A.; Nicholls, R. A.; Winn, M. D.; Long, F.; Vagin, A. A. *Acta Crystallogr., Sect. D: Biol. Crystallogr.* **2011**, *67*, 355.
(32) Emsley, P.; Cowtan, K. *Acta Crystallogr., Sect. D: Biol. Crystallogr.* **2004**, *60*, 2126.
(33) Laskowski, R. A.; Rullmannn, J. A.; MacArthur, M. W.; Kaptein, R.; Thornton, J. M. *J. Biomol. NMR* **1996**, *8*, 477.
(34) DeLano, W. L. *PYMOL*; DeLano Scientific: San Carlos, CA, 2002.

DOI: 10.1021/jacs.6b11258
J. Am. Chem. Soc. 2017, 139, 465−471